

Quantized Quadrupole Superconductors

Yun-Mei Li,^{1,*} Yongwei Huang,² and Kai Chang^{1,†}

¹*Center for Quantum Matter, School of Physics, Zhejiang University, Hangzhou 310027, China*

²*School of Physics, Ningxia University, Yinchuan 750021, China*

We introduce a class of superconductors termed “quantized quadrupole superconductors” that support Majorana corner modes according to the bulk-corner correspondence, distinct from previous works on the second-order topological superconductors. An intrinsic physical quantity for superconductors, i.e., the quadrupole moment serves as the topological invariant, which is always half-quantized due to the particle-hole symmetry. As examples, two types of mixed pairings, $d_{x^2-y^2} \pm id_{xy}$ and $d_{x^2-y^2} \pm is$, induced in the bilayer two-dimensional electron gases with Rashba spin-orbit coupling give the quadrupole phase. Extended discussions indicate that the nontrivial phase is robust against relative phase fluctuations in the mixed pairings and the disorders. Our schemes provide realistic platforms to implement Majorana zero modes, paving the way for studying the Majorana physics.

I. INTRODUCTION

Topological superconductors (TSCs) support Majorana excitations obeying non-Abelian exchange statistics, which are the key ingredient in topological quantum computations [1–6]. One of the key features in TSCs is the bulk-boundary correspondence [4, 5]. Usually, a nontrivial topological invariant derived from the bulk states under the assumptions of periodic boundary conditions (PBC) guarantees the emergence of localized Majorana modes at the boundaries (ends, edges or surfaces) when cutting the periodic systems along one certain direction [1, 5, 7–15]. The recognition of higher-order topology is expected to extend or enrich this correspondence [16–22]. The Majorana excitations appear at the intersections (corners or hinges) of adjacent boundaries when cutting the periodic system along two or three different directions in higher-order TSCs [21–34]. Part of the works utilize the crystalline symmetry analysis for the topological characterizations [19–22, 32]. However, this approach can not explain the persistence of the higher-order states when the related crystalline symmetries are broken. The others aim at gapping the first-order edge or surface states by in-plane magnetic fields [23–27] or unconventional superconductors [28–33]. The recent works [35, 36] attempt to connect the appearance of the Majorana corner modes to the bulk spectrum. However, the higher-order TSCs with bulk-boundary correspondence still remain unexplored.

In this Letter, we propose a class of superconductors dubbed as “quantized quadrupole superconductors” that support Majorana corner modes based on bulk-corner correspondence. By generalizing the quadrupole moment to the superconductors, we find that it is always half-quantized guaranteed only by the particle-hole symmetry in superconductors and thus behaves as an intrinsic physical quantity, different from that in electronic

systems relying on the crystalline symmetries. A one-half quadrupole moment implies the emergence of zero-energy corner modes in a square or rectangle sample under the open boundary condition (OBC), demonstrated to be Majorana corner modes (MCMs), also guaranteed by the particle-hole symmetry. Distinct from the previous works, our approach to the second-order TSCs only utilizes the particle-hole symmetry in superconductors, unique with requiring the minimal assumptions or conditions and revealing a new class of superconductors.

As concrete examples, we show that the bilayer spin-orbit coupled two-dimensional electron gases with at least two types of proximity pairings can host nontrivial quadrupole phase. The first pairing is the $d_{x^2-y^2} \pm id_{xy}$ ($d \pm id'$ for short) while the second is $d_{x^2-y^2} \pm is$ ($d \pm is$ for short). We take the twisted bilayer copper oxides to induce the $d \pm id'$ for calculations [37, 38]. The $d \pm is$ pairing can be realized by the Josephson junctions [39–42]. In the region where quadrupole moment does not vanish, there emerges single Majorana corner mode (MCM) at each corner under OBC. In the trivial region, the sample supports quasiparticle corner modes or no corner modes. The bulk gap closing and reopening give the phase transitions between the nontrivial and trivial region. The MCMs and bulk-corner correspondence in quadrupole superconductors are robust against the disorders. The quadrupole phase also survives from a large phase fluctuations in the mixed pairing. Besides, quadrupole superconductors are intrinsic higher-order TSCs, providing feasible schemes for experimentalists to achieve MCMs.

II. THE BULK QUADRUPOLE MOMENT IN SUPERCONDUCTORS

We establish the general theory of quantized quadrupole superconductors firstly. By generalizing Resta formula for electric polarization [43] and seminal works on the electric multipole insulators [44, 45], the quadrupole moment for superconductors is defined in the

* contact author:yunmeili@zju.edu.cn

† contact author:kchang@zju.edu.cn

real-space as

$$q_{xy} = \frac{1}{2\pi} \text{Im} \log[\det(\langle U | \hat{Q} | U \rangle)]. \quad (1)$$

$\hat{Q} = e^{2\pi i \hat{x} \hat{y} / (L_x L_y)}$. \hat{x} (\hat{y}) is the position operator along the x (y) dimension and $L_{x,y}$ the corresponding size. The matrix U is constructed by the quasiparticle states of negative energy branches obtained by diagonalizing the Bogoliubov-de Gennes (BdG) Hamiltonian. The quasiparticle eigenstates are defined on the torus with PBC such that only the bulk states determine the properties of q_{xy} . There is a reasonable rule on the operator \hat{Q} . For any spin, orbital and particle-hole degree of freedom on each site or coordinate, the position operator is adopted to be the same. When considering the spin and particle-hole degree of freedom, $\det(\hat{Q}) = 1$ in usual cases [46].

The particle-hole symmetry in superconductors guarantees that q_{xy} is always quantized to 0 or $\frac{1}{2}$ because $\det(U^\dagger \hat{Q} U)$ is real. The details are presented in the Supplementary Materials (SMs) [46]. We use Sylvester's determinant identity $\det(\mathbf{1} + AB) = \det(\mathbf{1} + BA)$ for the derivations. $\det(U^\dagger \hat{Q} U) = \det[U^\dagger (\hat{Q} - \mathbf{1} + \mathbf{1}) U] = \det[\mathbf{1} + (\hat{Q} - \mathbf{1}) U U^\dagger]$. Let V be the quasiparticle states of the positive energy branch. From the relation $U U^\dagger + V V^\dagger = \mathbf{1}$, we have

$$\det[\mathbf{1} + (\hat{Q} - \mathbf{1})(\mathbf{1} - V V^\dagger)] = \det(V^\dagger \hat{Q}^\dagger V). \quad (2)$$

Eq. (2) implies that $\det(U^\dagger \hat{Q} U) = \det(V^\dagger \hat{Q}^\dagger V)$. The particle-hole symmetry is usually of the form $\mathcal{P} = \tau_x \mathcal{K}$, relating U and V as $V = \mathcal{P}U = \tau_x U^*$, where τ_x acts on the particle-hole degree of freedom and \mathcal{K} denote the complex conjugation. Then $\det(V^\dagger \hat{Q}^\dagger V) = \det(U^T \tau_x \hat{Q}^\dagger \tau_x U^*) = [\det(U^\dagger \hat{Q} U)]^*$, indicates the half-quantization of q_{xy} . We here restrict $2q_{xy} = 1 \bmod 2$ to make $q_{xy} = 0$ or $\frac{1}{2}$.

The properties of the quadrupole moment for the two-dimensional (2D) superconductors are quite different from that for electronic systems. The half-quantization of q_{xy} in electronic systems [44, 45, 47, 48] relies on the mirror, four-fold rotational or chiral symmetries, which can be broken by the perturbations, such as the disorders, strains and other symmetry breaking terms. By contrast, the quadrupole moment for 2D superconductors behaves as an intrinsic physical quantity as its half-quantization is protected by the always present particle-hole symmetry in superconductors and is independent on the crystalline symmetries including the inversion symmetry [22]. The superconductors with $q_{xy} = \frac{1}{2}$ are expected to be robust against the above perturbations. More importantly, when $q_{xy} = \frac{1}{2}$, $\partial_x \partial_y q_{xy}$ is not zero only at the corners of a square or rectangle shaped sample under OBC, indicating the emergence of single zero-energy mode at each corner. These zero-energy states can be expressed as $\psi = \sum_i (u_i c_i + v_i c_i^\dagger)$, where i denote the combined orbital, spin and lattice index. Due to the particle-hole symmetry, we have $\psi = \mathcal{P}\psi = \sum_i (v_i^* c_i + u_i^* c_i^\dagger)$, making

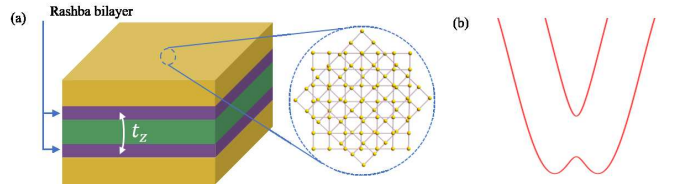


FIG. 1. (a) The illustration for the setup to achieve the first model for quadrupole superconductor that supports Majorana corner modes. The bilayer two-dimensional electron gases with Rashba spin-orbit coupling are in proximity to twisted bilayer copper oxides. The second model is by replacing the twisted bilayer copper oxides with Josephson junctions displaying $d \pm is$ pairings. (b) The bands for the bilayer 2DEGs near Γ point. The interlayer coupling t_z splits the two Rashba bands into bonding (lower) and antibonding states with a hybridization gap.

the relation $v_i = u_i^*$ and $\psi^\dagger = \psi$. The spatially separated zero-energy corner modes are thus Majorana corner modes. The quantized quadrupole superconductors then exhibit a bulk-corner correspondence.

III. REALISTIC EXAMPLES FOR QUANTIZED QUADRUPOLE SUPERCONDUCTORS

A. The electronic Hamiltonian

To obtain nontrivial quadrupole superconductors, the single-particle system is the coupled bilayer two-dimensional electron gases (2DEGs) with Rashba spin-orbit coupling (SOC), as illustrated in Fig. 1 (a). We note that the SOC in the bilayer 2DEGs are naturally opposite to each other due to the opposite structural asymmetry between the bottom and top layers. We employ a tight-binding Hamiltonian on a square lattice to describe the bilayer 2DEGs,

$$H_0 = \sum_{\langle ij \rangle, ss' \sigma} c_{i\sigma s}^\dagger [-t_0 \delta_{ss'} + i\alpha \sigma_z (\mathbf{s} \times \hat{\mathbf{d}}_{ij})_z] c_{j\sigma s'} + H_z, \quad (3)$$

where $H_z = t_z \sum_{is, \sigma \neq \sigma'} c_{i\sigma s}^\dagger c_{i\sigma' s'}$ is the tunneling term between the two layers. $\hat{\mathbf{d}}_{ij}$ is the unit vector pointing from site i to site j . \mathbf{s} and σ denote the spin and layer indices, respectively. α characterizes the strength of the SOC. With a Fourier transformation to the momentum space, $H_0 = \sum_{\mathbf{k}} \psi_{\mathbf{k}}^\dagger h_{\mathbf{k}} \psi_{\mathbf{k}}$ in the basis of $\psi_{\mathbf{k}} = (c_{\mathbf{k},1\uparrow}, c_{\mathbf{k},1\downarrow}, c_{\mathbf{k},2\uparrow}, c_{\mathbf{k},2\downarrow})^T$, where

$$h_{\mathbf{k}} = \xi_{\mathbf{k}} + 2\alpha(s_x \sin k_y - s_y \sin k_x) \sigma_z + t_z \sigma_x, \quad (4)$$

and $\xi_{\mathbf{k}} = -2t_0(\cos k_x + \cos k_y - 2)$. The 2 in the bracket of $\xi_{\mathbf{k}}$ is for resetting the zero energy position. The interlayer coupling hybridize the two Rashba bands at the top and bottom layers with a gap $2t_z$ at Γ [$\mathbf{k} = (0, 0)$] and M [$\mathbf{k} = (\pi, \pi)$] points, as illustrated in Fig. 1 (b).

B. $d \pm id'$ proximity pairing

There are many ways to induce the $d \pm id'$ proximity paring in the 2DEGs [38, 49, 50]. We choose the twisted bilayer copper oxides proposed in the recent work [38] to proximitize the 2DEGs inducing our desired mixed pairing, as illustrated in Fig. 1 (a). One of the candidate materials is the van der Waals-bonded high-critical-temperature copper oxide materials, such as $\text{Bi}_2\text{Sr}_2\text{CaCu}_2\text{O}_{8+\delta}$ (Bi2212), which gives $d_{x^2-y^2}$ pairing upon a high critical temperature $T_c \simeq 90$ K. When the twist angle $\theta \simeq 45^\circ$, the relative phase between two layers is about $\pm\pi/2$ to generate $d \pm id'$ pairing. The relative phase would spontaneously choose one of the two values [38]. For simplicity, we here restrict the bottom (top) 2DEG layer are in proximity contact to the twisted bilayer cooper oxides with the relative phase $\pi/2$ ($-\pi/2$) or vice versa, achievable experimentally by proper choosing the twisted samples or phase locking techniques. The case for other twist angles and relative phases will be discussed at the end. We can express the proximity superconducting pairing in the Rashba bilayer as

$$H_{\Delta}^a = \sum_{\sigma=1}^2 [i\Delta'\sigma_z(\sum_{\langle\langle ij \rangle\rangle_1} c_{i\sigma\uparrow}^\dagger c_{j\sigma\downarrow}^\dagger - \sum_{\langle\langle ij \rangle\rangle_2} c_{i\sigma\uparrow}^\dagger c_{j\sigma\downarrow}^\dagger) + \Delta(\sum_{\langle ij \rangle_{\hat{x}}} c_{i\sigma\uparrow}^\dagger c_{j\sigma\downarrow}^\dagger - \sum_{\langle ij \rangle_{\hat{y}}} c_{i\sigma\uparrow}^\dagger c_{j\sigma\downarrow}^\dagger) + H.c.], \quad (5)$$

$\langle ij \rangle_{\hat{x}(\hat{y})}$ denotes the nearest neighbor along the x (y) direction. $\langle\langle ij \rangle\rangle_1$ ($\langle\langle ij \rangle\rangle_2$) denotes the second nearest neighbor along the $\hat{x} + \hat{y}$ ($\hat{x} - \hat{y}$) direction.

The total Hamiltonian in the BdG formalism under the basis $\Psi_{\mathbf{k}} = (\psi_{\mathbf{k}}, \psi_{-\mathbf{k}}^\dagger)^T$ is given by

$$H_{\text{BdG}}^a(\mathbf{k}) = \begin{pmatrix} h_{\mathbf{k}} - \mu & \Delta_{\mathbf{k}a} \\ \Delta_{\mathbf{k}a}^\dagger & -h_{-\mathbf{k}}^* + \mu \end{pmatrix}, \quad (6)$$

where μ is the chemical potential and $\Delta_{\mathbf{k}a} = i\Delta_{\mathbf{k}}^1 s_y \sigma_0 - \Delta_{\mathbf{k}}^2 s_y \sigma_z$ with $\Delta_{\mathbf{k}}^1 = 2\Delta(\cos k_x - \cos k_y)$ and $\Delta_{\mathbf{k}}^2 = 4\Delta' \sin k_x \sin k_y$. The doubly degenerate quasiparticle spectrum $E = \pm\sqrt{A \pm 2\sqrt{B}}$ with $A = (\xi_{\mathbf{k}} - \mu)^2 + 4\alpha^2(\sin^2 k_x + \sin^2 k_y) + t_z^2 + (\Delta_{\mathbf{k}}^1)^2 + (\Delta_{\mathbf{k}}^2)^2$ and $B = (\xi_{\mathbf{k}} - \mu)^2[t_z^2 + 4\alpha^2(\sin^2 k_x + \sin^2 k_y)] + t_z^2(\Delta_{\mathbf{k}}^2)^2$. We can see the bulk spectrum is fully gapped except when $\mu = \pm t_z, 8t_0 \pm t_z$, which will be shown later, are the phase transition points. The system holds no time-reversal symmetry (TRS) but preserves a particle-hole symmetry $\mathcal{P} = \tau_x \mathcal{K}$: $\mathcal{P} H_{\text{BdG}}^a(\mathbf{k}) \mathcal{P}^{-1} = -H_{\text{BdG}}(-\mathbf{k})$. A nontrivial value of q_{xy} demands gapped bulk and edge spectrum simultaneously.

We employ the tight-binding Hamiltonian presented in Eq. (2) and Eq. (4) to calculate the quasiparticle energy spectrum for one-dimensional ribbon to check the existence of edge gap. The quasiparticle bands for a x -directional ribbon are shown in Fig. 2 (a) with chemical potential $\mu = 0$. A clear edge gap can be seen. At

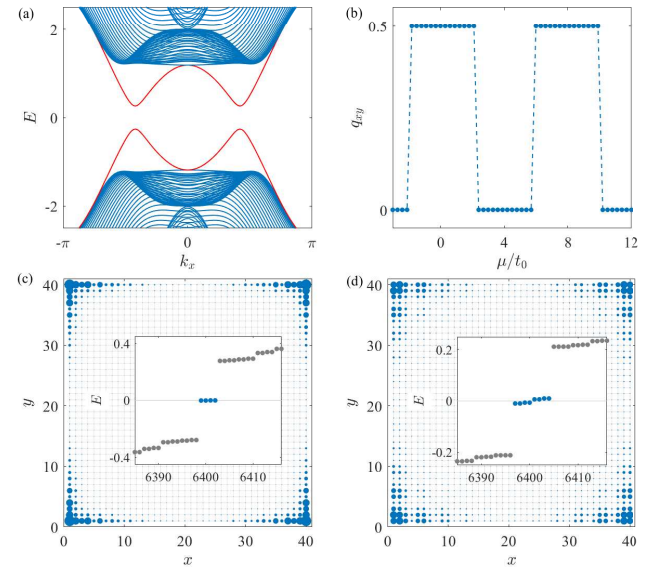


FIG. 2. (a) The quasiparticle dispersions for a ribbon along the x direction when the Fermi energy $\mu = 0$. The ribbon width is adopted $N_y = 40$. (b) The quadrupole moment q_{xy} with respect to μ . The sample size is chosen as 40×40 for the calculations. (c)-(d) Density distribution for the corner modes with the two chemical potential $\mu = 0$ and $\mu = 4.0$, respectively. The insets show the energy levels around the zero energy. The sample size is 40×40 . In all the panels, $t_0 = 1.0$, $\alpha = 1.0$, $t_z = 2.0$, $\Delta = 0.5$, $\Delta' = 0.4$.

other chemical potentials the edge gap always presents even when the bulk gap closes at $\mu = \pm t_z, 8t_0 \pm t_z$ [46]. The quadrupole moment q_{xy} with respect to the chemical potential μ is shown in Fig. 2 (b). In the ranges $-t_z < \mu < t_z$ and $8t_0 - t_z < \mu < 8t_0 + t_z$, q_{xy} is $1/2$. In these ranges, the Fermi level only crosses the bonding or antibonding bands. The phase transitions are accompanied by the bulk gap closing and reopening.

To demonstrate the bulk-corner correspondence, we calculate quasiparticle energy level in a square-shaped sample at different μ under OBC. The results are shown in Figs. 2 (c) and 2 (d). When μ is in the region giving nontrivial q_{xy} , four MCMs localize at the four corners separately [Fig. 2 (c)]. Due to the high critical temperature superconductors we adopted ($T_c \simeq 90$ K for Bi2212), these Majorana corner modes are expected to survive up to a very high temperature. When μ locates in the trivial region, we find eight quasiparticle corner modes with nonzero energy. There are only four independent physical corner modes while the other four are related by the particle-hole symmetry [Fig. 2 (d)]. The energies of these corner modes do not approach to zero at sufficiently large sample size [46], demonstrated that they are not MCMs.

C. $d \pm is$ proximity pairing

Another type of proximity pairing, i.e., $d \pm is$ can also induce a nontrivial quadrupole phase. We replace the twisted bilayer copper oxides with a hybrid Josephson junctions consisting of cuprate superconductors and conventional s-wave superconductors. We here suppose a relative $\pm \frac{\pi}{2}$ phase between the two different pairings. Similarly, we restrict the bottom (top) 2DEG layer to acquire a $d + is$ ($d - is$) proximity superconducting pairing. The induced proximity interaction in 2DEGs can be described as

$$H_{\Delta}^b = \sum_{\sigma=1}^2 [\Delta (\sum_{\langle ij \rangle_x} c_{i\sigma\uparrow}^\dagger c_{j\sigma\downarrow}^\dagger - \sum_{\langle ij \rangle_y} c_{i\sigma\uparrow}^\dagger c_{j\sigma\downarrow}^\dagger) + i\Delta_0 \sigma_z \sum_i c_{i\sigma\uparrow}^\dagger c_{i\sigma\downarrow}^\dagger + H.c.]. \quad (7)$$

The BdG formalism of Hamiltonian can be obtained by replacing Δ_{ka} in Eq. (6) with $\Delta_{kb} = 2i\Delta(\cos k_x - \cos k_y)s_y\sigma_0 - \Delta_0s_y\sigma_z$. The quasiparticle eigenvalues $E = \pm\sqrt{A' \pm 2\sqrt{B'}}$ with $A' = (\xi_{\mathbf{k}} - \mu)^2 + 4\alpha^2(\sin^2 k_x + \sin^2 k_y) + t_z^2 + (\Delta_{\mathbf{k}}^1)^2 + \Delta_0^2$ and $B' = (\xi_{\mathbf{k}} - \mu)^2[t_z^2 + 4\alpha^2(\sin^2 k_x + \sin^2 k_y)] + t_z^2\Delta_0^2$. The quasiparticle gap closes when $t_z = \pm\sqrt{\mu^2 + \Delta_0^2}$ or $t_z = \pm\sqrt{(\mu - 8t_0)^2 + \Delta_0^2}$. The particle-hole symmetry $\mathcal{P} = \tau_x\mathcal{K}$ is preserved but the TRS is also broken. We present the phase diagram, i.e., quadrupole moment q_{xy} with respect to t_z and μ in Fig. 3 (a). In the regions $|t_z| > \sqrt{\mu^2 + \Delta_0^2}$ and $|t_z| > \sqrt{(\mu - 8t_0)^2 + \Delta_0^2}$, q_{xy} is 1/2, indicating the emergence of the MCMs. In real systems, we should consider the μ dependence of proximity pairing [51]. Simply replacing Δ_0 with $\Delta_0(\mu)$ could simulate the realistic situations. The energy levels of a squared sample and the density distribution of the zero-energy corner states are shown in Fig. 3 (b).

IV. RELEASE OF EXPERIMENTAL CONDITIONS

The recent experiments have successfully fabricated the twisted bilayer cuprates [52, 53] with multiple twist angles. The phenomena related with the TRS breaking are observed. The hybrid Josephson junctions consisting of cuprate superconductors and conventional s-wave superconductors have also been successfully fabricated experimentally and well studied decade ago [39–41]. The two setups we proposed are experimentally achievable. We adopt the specific $\pm \frac{\pi}{2}$ relative phase to simplify our calculations and discussions. We show that the nontrivial quadrupole phase survives to a very large range of the relative phase.

As discussed in Ref. [38], gapped superconducting phase survives between the critical values of the twist angle of the bilayer cuprate superconductors. For the first

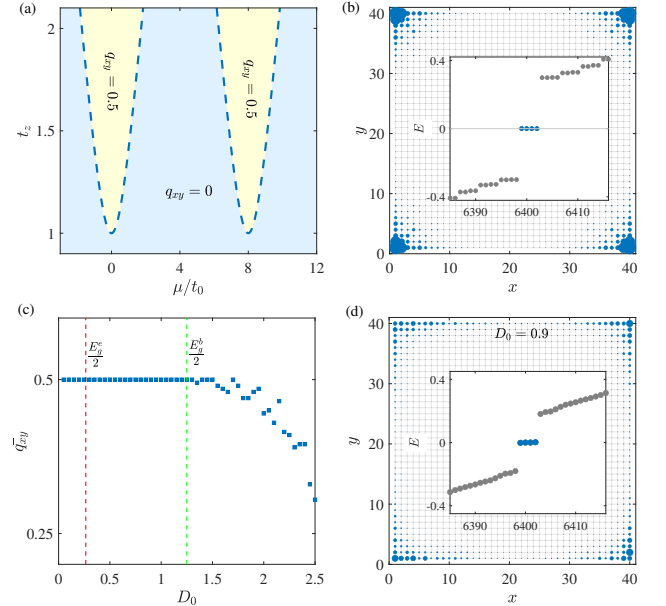


FIG. 3. (a) The phase diagram in the $t_z - \mu$ plane. The sample size is adopted as 20×20 for the numerical calculations of q_{xy} . The dashed lines are the phase boundary obtained analytically from the band gap closing condition. (b) Density distribution of the MCMs with $\mu = 0$ and $t_z = 2.0$. The inset shows the energy levels around the zero energy. The sample size is adopted as 40×40 . (c) The averaged q_{xy} with respect to the disorder strength D_0 for the first model. E_g^e denotes the edge gap while E_g^b denotes the bulk gap of quasiparticles. (d) The spatial distributions of the MCMs at disorder strength $D_0 = 0.9$ for the first model.

setup, the requirements are that the twist angle is also between the critical values $\theta_c^- < \theta < \theta_c^+$ and the sign of the relative phase for the bottom and top bilayer cuprates are opposite. The twist angles and the pairing amplitudes for the top and bottom bilayer cuprates do not need to be same. To perform the calculations, we firstly express the proximity pairing term in a continuous form for any angle, $\Delta_{\mathbf{k}}^\sigma = \Delta(k_y^2 - k_x^2) + \Delta' e^{i\varphi(\theta_\sigma)} [(k_y')^2 - (k_x')^2]$, where $(k_x', k_y')^\top = R(\theta)(k_x, k_y)^\top$ and $R(\theta)$ is the 2D representation of $SO(2)$ rotation group. The phase $\varphi(\theta)$ can be calculated from the twist angle and material parameters [38, 46]. Then we map $\Delta_{\mathbf{k}}^\sigma$ on the square lattice. The detailed calculations are presented in the SMs [46], presenting same results to Fig. 2 even we adopt different twist angles between top and bottom bilayer. For the second setup, the nontrivial quadrupole phase survives at a large area of the relative phase between the d -wave and s-wave pairings. We present the detailed results in the SMs [46].

Besides, we would like to mention that the bilayer 2DEGs can be replaced by a thin film of 3D strong topological insulators. The surface states on opposite surface have opposite helicity, perfectly coincides with the Rashba bilayer system. Our proposal does not require

precise square sample, either. See SMs for the MCMs in other geometries [46].

V. DISORDERS

We turn to the disorder effects. The disorders break all the crystalline symmetries, including the mirror, rotational and inversion symmetries. There are at least two sources of disorders, coming from the single-particle and the pairings, respectively. We take the first model for the discussions. The phase diagram in Fig. 2 (b) depends only on the chemical potential. The nontrivial phase is robust against on the proximity pairing amplitude fluctuations. Meanwhile, we do not need to consider the chemical dependence of the proximity pairing amplitude.

For the disorders coming from the electronic states, we consider the random on-site disorders. The disorder Hamiltonian reads

$$H_{dis} = \sum_{i\sigma} c_{i\sigma}^\dagger V_{i\sigma} c_{i\sigma}. \quad (8)$$

The random potential $V_{i\sigma}$ obeys a Gaussian distribution, namely $\langle V_{i\sigma} \rangle = 0$, $\langle V_{i\sigma} V_{j\sigma'} \rangle = D_0^2 \delta_{ij} \delta_{\sigma\sigma'}$, with D_0 characterizing the strength of the random disorders. Since the q_{xy} is still half-quantized in the presence of the disorders, we apply 100 different disorder configurations to average the q_{xy} to study the robustness of the MCMs. The results are presented in Fig. 3 (c). The q_{xy} is robust even when the disorder strength is much larger than the edge gap. Only when $2D_0$ is larger than the bulk gap, the disorders could destroy the bulk-corner correspondence and the MCMs. We present the MCMs in Fig. 3 (d) un-

der a strong disorder configuration. These behaviors are natural result due to the bulk protection.

VI. DISCUSSIONS AND SUMMARY

We only discuss the quantized quadrupole phase in 2D systems. Direct extension to the 3D systems could predict the quantized octupole superconductors. The octupole moment can be defined similar to Eq. (1), with $\hat{Q} = e^{2\pi i \hat{x}\hat{y}\hat{z}/(L_x L_y L_z)}$. The realistic systems that exhibit the octupole phase will be discussed in the future.

In summary, we established the higher-order topological superconductors protected by bulk quadrupole moment. These superconductors are robust against the phase fluctuations of the mixed pairing in realistic systems and also the disorders. Together with the intrinsic nature, the models we proposed are experimentally feasible by current techniques, providing alternative platforms for the study of the Majorana excitations and non-Abelian statistics in condensed matter systems.

ACKNOWLEDGEMENTS

Y.-M. Li thanks Prof. Xiancong Lu and Prof. Wei-Nan Lin for their helpful discussions. Y.-M. Li acknowledges the support from NSFC under Grant No. 12474050 and the MOST of China under Grant No. 2022YFA1204700. K. Chang acknowledges the support from NSFC under Grant No. 12488101. Y. Huang acknowledges the support from NSFC under Grant No. 12304107 and the key research and development project of Ningxia under Grants No. 2022BSB03095.

-
- [1] A. Yu Kitaev, Unpaired Majorana fermions in quantum wires, *Phys. Usp.* **44**, 131 (2001).
- [2] A. Yu Kitaev, Fault-tolerant quantum computation by anyons, *Ann. Phys. (Amsterdam)* **303**, 2 (2003).
- [3] C. Nayak, S. H. Simon, A. Stern, M. Freedman, and S. D.Sarma, Non-Abelian anyons and topological quantum computation, *Rev. Mod. Phys.* **80**, 1083 (2008).
- [4] M. Z. Hasan and C. L. Kane, Colloquium: Topological insulators, *Rev. Mod. Phys.* **82**, 3045 (2010).
- [5] X.-L. Qi and S.-C. Zhang, Topological insulators and superconductors, *Rev. Mod. Phys.* **83**, 1057 (2011).
- [6] S. R. Elliott and M. Franz, Colloquium: Majorana fermions in nuclear, particle, and solid-state physics, *Rev. Mod. Phys.* **87**, 137 (2015).
- [7] C. Zhang, S. Tewari, R. M. Lutchyn, and S. Das Sarma, $p_x + ip_y$ superfluid from s -wave interactions of fermionic cold atoms, *Phys. Rev. Lett.* **101**, 160401 (2008).
- [8] J. Alicea, New directions in the pursuit of Majorana fermions in solid state systems, *Rep. Prog. Phys.* **75**, 076501 (2012).
- [9] T. D. Stanescu and S. Tewari, Majorana fermions in semiconductor nanowires: Fundamentals, modeling, and experiment, *J. Phys.: Condens. Matter* **25**, 233201 (2013).
- [10] C. Beenakker, Search for majorana fermions in superconductors, *Annu. Rev. Condens. Matter Phys.* **4**, 113 (2013).
- [11] Y. Oreg, G. Refael, and F. von Oppen, Helical liquids and majorana bound states in quantum wires, *Phys. Rev. Lett.* **105**, 177002 (2010).
- [12] R. M. Lutchyn, J. D. Sau, and S. Das Sarma, Majorana fermions and a topological phase transition in semiconductor-superconductor heterostructures, *Phys. Rev. Lett.* **105**, 077001 (2010).
- [13] S. Tewari and J. D. Sau, Topological invariants for spin-orbit coupled superconductor nanowires, *Phys. Rev. Lett.* **109**, 150408 (2012).
- [14] Sho Nakosai, Yukio Tanaka, and Naoto Nagaosa, Topological superconductivity in bilayer rashba system, *Phys. Rev. Lett.* **108**, 147003 (2012).
- [15] F. Zhang, C. L. Kane, and E. J. Mele, Time-reversal-invariant topological superconductivity and majorana kramers pairs *Phys. Rev. Lett.* **111**, 056402 (2013).
- [16] W. A. Benalcazar, B. Andrei Bernevig, T. L. Hughes, Quantized electric multipole insulators,

- Science **357**, 61 (2017).
- [17] W. A. Benalcazar, B. A. Bernevig, and T. L. Hughes, Electric multipole moments, topological multipole moment pumping, and chiral hinge states in crystalline insulators, *Phys. Rev. B* **96**, 245115 (2017).
- [18] Y.-M. Li, Y.-J. Wu, X.-W. Luo, Y. Huang, and K. Chang, Higher-order topological phases of magnons protected by magnetic crystalline symmetries, *Phys. Rev. B* **106**, 054403 (2022).
- [19] J. Langbehn, Y. Peng, L. Trifunovic, F. von Oppen, and P. W. Brouwer, Reflection-symmetric second-order topological insulators and superconductors, *Phys. Rev. Lett.* **119**, 246401 (2017).
- [20] Z. Song, Z. Fang, and C. Fang, $(d-2)$ -dimensional edge states of rotation symmetry protected topological states, *Phys. Rev. Lett.* **119**, 246402 (2017).
- [21] M. Geier, L. Trifunovic, M. Hoskam, and P. W. Brouwer, Second-order topological insulators and superconductors with an order-two crystalline symmetry, *Phys. Rev. B* **97**, 205135 (2018).
- [22] E. Khalaf, Higher-order topological insulators and superconductors protected by inversion symmetry, *Phys. Rev. B* **97**, 205136 (2018).
- [23] X. Zhu, Tunable Majorana corner states in a two-dimensional second-order topological superconductor induced by magnetic fields, *Phys. Rev. B* **97**, 205134 (2018).
- [24] Y. Volpez, D. Loss, and J. Klinovaja, Second-order topological superconductivity in π -junction Rashba layers, *Phys. Rev. Lett.* **122**, 126402 (2019).
- [25] Y.-J. Wu, J. Hou, Y.-M. Li, X.-W. Luo, X. Shi, and C. Zhang, In-plane Zeeman-field-induced Majorana corner and hinge modes in an s-wave superconductor heterostructure, *Phys. Rev. Lett.* **124**, 227001 (2020).
- [26] A. K. Ghosh, T. Nag, and A. Saha, Floquet generation of a second-order topological superconductor, *Phys. Rev. B* **103**, 045424 (2021).
- [27] Y.-X. Li and C.-C. Liu, High-temperature Majorana corner modes in a $d \pm id'$ superconductor heterostructure: Application to twisted bilayer cuprate superconductors, *Phys. Rev. B* **107**, 235125 (2023).
- [28] Z. Yan, F. Song, and Z. Wang, Majorana corner modes in a high-temperature platform, *Phys. Rev. Lett.* **121**, 096803 (2018).
- [29] Q. Wang, C.-C. Liu, Y.-M. Lu, and F. Zhang, High-temperature Majorana corner states, *Phys. Rev. Lett.* **121**, 186801 (2018).
- [30] X. Zhu, Second-order topological superconductors with mixed pairing, *Phys. Rev. Lett.* **122**, 236401 (2019).
- [31] R.-X. Zhang, W. S. Cole, and S. Das Sarma, Helical hinge Majorana modes in iron-based superconductors, *Phys. Rev. Lett.* **122**, 187001 (2019).
- [32] Z. Yan, Higher-order topological odd-parity superconductors, *Phys. Rev. Lett.* **123**, 177001 (2019).
- [33] Y.-T. Hsu, W. S. Cole, R.-X. Zhang, and J. D. Sau, Inversion-protected higher-order topological superconductivity in monolayer WTe₂, *Phys. Rev. Lett.* **125**, 097001 (2020).
- [34] A. Chew, Y. Wang, B. A. Bernevig, and Z.-D. Song, Higher-order topological superconductivity in twisted bilayer graphene, *Phys. Rev. B* **107**, 094512 (2023).
- [35] H. Wang and X. Zhu, Higher-order topological superconductors characterized by Fermi level crossings, *Phys. Rev. B* **108**, 125426 (2023).
- [36] X. Zhu, Direct demonstration of bulk-boundary correspondence in higher-order topological superconductors with chiral symmetry, *Phys. Rev. B* **110**, 075103 (2024).
- [37] Y. Yu, L. Ma, P. Cai, R. Zhong, C. Ye, J. Shen, G. D. Gu, X. Hui Chen, and Y. Zhang, High-temperature superconductivity in monolayer Bi₂Sr₂CaCu₂O_{8+δ}, *Nature* **575**, 156 (2019).
- [38] O. Can, T. Tummuru, R. P. Day, I. Elfimov, A. Damascelli, and M. Franz, High-temperature topological superconductivity in twisted double-layer copper oxides, *Nat. Phys.* **17**, 519 (2021).
- [39] R. Kleiner, A. S. Katz, A. G. Sun, R. Summer, D. A. Gajewski, S. H. Han, S. I. Woods, E. Dantsker, B. Chen, K. Char, M. B. Maple, R. C. Dynes, and John Clarke, Pair tunneling from c-axis YBa₂Cu₃O_{7-x} to Pb: evidence for s-wave component from microwave induced steps, *Phys. Rev. Lett.* **76**, 2161 (1996).
- [40] P. V. Komissinski, E. Illichev, G. A. Ovsyannikov, S. A. Kovtonyuk, M. Grajcar, R. Hlubina, Z. Ivanov, Y. Tanaka, N. Yoshida, and S. Kashiwaya, Observation of the second harmonic in superconducting current-phase relation of Nb/Au/(001)YBa₂Cu₃O_x heterojunctions, *Europhys. Lett.* **57**, 585 (2002).
- [41] P. Komissinskiy, G. A. Ovsyannikov, I. V. Borisenko, Yu. V. Kislinskii, K. Y. Constantinian, A. V. Zaitsev, and D. Winkler, Josephson Effect in Hybrid Oxide Heterostructures with an Antiferromagnetic Layer, *Phys. Rev. Lett.* **99**, 017004 (2007).
- [42] S. Charpentier, G. Roberge, S. Godin-Proulx, P. Fournier, Proximity effect in electron-doped cuprate Josephson junctions, *Appl. Phys. Lett.* **99**, 032511 (2011).
- [43] R. Resta, Quantum-mechanical position operator in extended systems, *Phys. Rev. Lett.* **80**, 1800 (1998).
- [44] W. A. Wheeler, L. K. Wagner, and T. L. Hughes, Many-body electric multipole operators in extended systems, *Phys. Rev. B* **100**, 245135 (2019).
- [45] B. Kang, K. Shiozaki, and G. Young Cho, Many-body order parameters for multipoles in solids, *Phys. Rev. B* **100**, 245134 (2019).
- [46] See Supplemental Material at [url], which includes Refs [38], for details of (Sec. S1) proof of the quantization of quadrupole moments protected by particle-hole symmetry, (Sec. S2) gapped edge states of the first model, (Sec. S3) the corner modes in the trivial region, (Sec. S4) the Majorana corner modes at other twist angles, (Sec. S5) $d \pm is$ pairing, (Sec. S6) Majorana corner modes at other geometries, (Sec. S7) quantized octupole superconductors.
- [47] S. Ono, L. Trifunovic, and H. Watanabe, Difficulties in operator-based formulation of the bulk quadrupole moment, *Phys. Rev. B* **100**, 245133 (2019).
- [48] Y. Tada and M. Oshikawa, Many-body multipole index and bulk-boundary correspondence, *Phys. Rev. B* **108**, 235150 (2023).
- [49] R. B. Laughlin, Magnetic induction of $d_{x^2-y^2} + id_{xy}$ order in high- T_c superconductors, *Phys. Rev. Lett.* **80**, 5188 (1998).
- [50] Z. Yang, S. Qin, Q. Zhang, C. Fang, and J. Hu, $\pi/2$ -Josephson junction as a topological superconductor, *Phys. Rev. B* **98**, 104515 (2018).
- [51] A. M. Black-Schaffer, Edge Properties and Majorana Fermions in the Proposed Chiral d -Wave Superconducting State of Doped Graphene,

- [Phys. Rev. Lett. **109**, 197001 \(2012\)](#).
- [52] Y. Zhu, M. Liao, Q. Zhang, H.-Y. Xie, F. Meng, Y. Liu, Z. Bai, S. Ji, J. Zhang, K. Jiang, R. Zhong, J. Schneeloch, G. Gu, L. Gu, X. Ma, D. Zhang, and Q.-K. Xue, Presence of *s*-wave pairing in Josephson junctions made of twisted ultrathin $\text{Bi}_2\text{Sr}_2\text{CaCu}_2\text{O}_{8+x}$ flakes, [Phys. Rev. X **11**, 031011 \(2021\)](#).
- [53] S. Y. Frank Zhao, X. Cui, P. A. Volkov, H. Yoo, S. Lee, J. A. Gardener, A. J. Akey, R. Engelke, Y. Ronen, R. Zhong, G. Gu, S. Plugge, T. Tummuru M. Kim, M. Franz, J. H. Pixley, N. Poccia, P. Kim, Time-reversal symmetry breaking superconductivity between twisted cuprate superconductors, [Science **382**, 1422 \(2023\)](#).